Articles

Theoretical Study on Intermolecular Interactions and Thermodynamic Properties of Dimethylnitroamine Clusters

JU, Xue-Hai(居学海)   XIAO, He-Ming*(肖鹤鸣)   TAN, Jin-Zhi(潭金芝)

Department of Chemistry, Nanjing University of Science and Technology, Nanjing 210094, China

Ab initio SCF and Møller-Plesset correlation correction methods in combination with counterpoise procedure for BSSE correction have been applied to the theroetical studying of dimethylnitroamine and its dimers and trimers. Three optimized stable dimers and two trimers have been obtained. The corrected binding energies of the most stable dimer and trimer were predicted to be − 24.68 kJ/mol and − 47.27 kJ/mol, respectively at the MP2/6-31G*//HF/6-31G* level. The proportion of correlated interaction energies to their total interaction energies for all clusters was at least 29.3 percent, and the BSSE of ΔE(MP2) was at least 10.0 kJ/mol. Dispersion and/or electrostatic force were dominant in all clusters. There exist cooperative effects in both the chain and the cyclic trimers. The vibrational frequencies associated with N—O stretches or wags exhibit slight red shifts, but the modes associated with the motion of hydrogen atoms of the methyl group show somewhat blue shifts with respect to those of monomer. Thermodynamic properties of dimethylnitroamine and its clusters at different temperatures have been calculated on the basis of vibrational analyses. The changes of the Gibbs free energies for the aggregation from monomer to the most stable dimer and trimer were predicted to be 14.37 kJ/mol and 30.40 kJ/mol, respectively, at 1 atm and 298.15 K.

Keywords   dimethylnitroamine cluster, intermolecular interaction, *ab initio*, thermodynamic property

Introduction

Theoretical treatment of intermolecular interactions is emphasized by the fact that despite an enormous progress in various experimental techniques the unambiguous description of such process is still impractical. The binding energies of intermolecular interactions are much less than those of chemical bonding, and yet they play significant roles in a wide range of physical, chemical and biological fields. Researches on the weak interactions began with hydrogen bonds. Scheiner summarized in details the *ab initio* investigations on hydrogen bonding.[1] Based on the basis set improving and basis set superposition error (BSSE) correcting, the Møller-Plesset perturbation theory could predict supermolecular structures and binding energies not only for H-bonded systems but also for other systems.[2-7] In recent years, we have investigated the intermolecular interactions of energetic systems and obtained some meaningful information[8-13] that will be helpful to the study and the molecular design of energetic compounds. The behavior of molecular clusters is usually between two extremes: the gas phase and the crystal solid phase. Consequently, one can obtain valuable knowledge about the transition state of these extremes by examining the properties of clusters of large size. Clusters containing more than two molecules behave cooperative effects,[7,14] which are reflected in changes of some properties such as the increase of interaction intensity and the frequency shift with increase in cluster size. Thus properly characterizing these phenomena is crucial to understanding the behavior of cluster.

Dimethylnitroamine (DMNA) is a simple model of nitramine energetic compounds such as cyclotetramethylene-tetranitramine (HMX) and cyclotrimethylene-trinitramine (RDX) that are especially used as explosives. Researches already have done only focus on its

monomer.[15-21] The intermolecular forces control such diverse phenomena as the diffusion, the aggregation and the detonation. To provide the fundamental information for further investigation on the mixture explosives containing nitroamines, it is particularly necessary to study the intermolecular interaction. The aim of this paper is to theoretically investigate the structures, the IR shifts, the binding energies, the cooperativity effects and the thermodynamic properties of DMNA clusters by *ab initio* method. Natural bond orbital (NBO) and Mulliken population analyses were performed to probe the origin of the interaction.

Computational Methods

DMNA monomer and all its possible stable dimers and trimers obtained from Chem3D software are fully optimized at the HF/6-31G* level by the Berny method.[22,23] Natural bond orbital analyses and frequency calculations were performed on each optimized structure. Thermodynamic properties and their changes in the aggregation are derived from statistical thermodynamics based on the frequencies.

The interaction energy of complex is evaluated as the sum of the HF interaction energy and the correlation interaction energy. On condition that the latter term is determined by the Møller-Plesset perturbation theory,[24-26] the interaction energy is calculated as:

$$\Delta E(\mathrm{MP}) = \Delta E^{\mathrm{HF}} + \Delta E^{\mathrm{MP}}$$

where ΔE^{HF} is the HF interaction energy, ΔE^{MP} is the correlation interaction energy given by the MP calculation. The basis sets commonly used to calculate the energies in the above equation are far from being saturated and, hence, in any complex each subsystem will tend to lower its energy by using the basis functions of the other subsystem. The energies obtained at the equilibrium geometry of the complex for each subsystem are lower than those calculated at the same geometry with the basis functions of the respective subsystem alone. This energy difference is the so-called BSSE that can be checked by Boys and Bernardi's counterpoise procedure (CP).[27-29] For complex of two submolecules the BSSE is:

$$\mathrm{BSSE} = \mathrm{BSSE(A)} + \mathrm{BSSE(B)}$$
$$= \{E(\mathrm{A}) - E(\mathrm{A[B]})\} + \{E(\mathrm{B}) - E(\mathrm{B[A]})\}$$

where the $E(\mathrm{A[B]})$ and $E(\mathrm{B[A]})$ are the energies of A

and B, respectively, when the other subsystem's basis sets are added. Then the corrected interaction energy is:

$$\Delta E(\mathrm{MP})_{\mathrm{C}} = \Delta E_{\mathrm{C}}^{\mathrm{HF}} + \Delta E_{\mathrm{C}}^{\mathrm{MP}} = \Delta E(\mathrm{MP}) + \mathrm{BSSE}$$

The effects of cooperativity in the interaction could be estimated from various parameters such as structural changes undergone by clustering and the shifts in some vibrational frequencies. The more direct evaluation of the contributions of cooperativity in this paper is obtained by comparing the interaction energy of the cluster with the pairwise interaction energies calculated with the whole basis sets for the cluster in order to exclude BSSE.[6,7,14] Thus, for trimer the cooperativity contribution is:

$$E_{\mathrm{nopair}} = \Delta E_{\mathrm{ABC}}(\mathrm{ABC}) - \Delta E_{\mathrm{AB}}(\mathrm{ABC})$$
$$- \Delta E_{\mathrm{AC}}(\mathrm{ABC}) - \Delta E_{\mathrm{BC}}(\mathrm{ABC})$$

where terms in brackets mean that the whole basis sets for the cluster is used in calculations.

All calculations were performed with Gaussian98 program[30] on a Compaq Alpha600 Workstation in our laboratory.

Results and discussion

Optimized geometries

Fig. 1 shows the stable structures of DMNA and its clusters. Table 1 lists some optimized geometrical parameters at the HF/6-31G* level for DMNA and its clusters. The monomer has C_s symmetry with N—NO$_2$ coplanar and the carbon atoms C(5) and C(6) out of the plane. These results are in good agreement with all previous theory work or with low temperature crystalline form, but differ from the experimental gas-phase geometry of C_{2v} symmetry.[31,32] This discrepancy is due to that the planar or pyramidal nature of amino group is sufficiently weak and capable of altering the geometry.[21] A four- or eight-numbered ring between two submolecules is formed in each dimer, and a four- or six-numbered ring in trimer. The minimal intermolecular distances are in the order: **IIa** (0.2811 nm) > **IIb** (0.2675 nm)—**IIc** (0.2678 nm) > **IIIa** (0.2637 nm)—**IIIb** (0.2642 nm). From the intermolecular distances and the O⋯H contacting numbers, it can be deduced that the magnitudes of interactions may be **IIa**—**IIb** < **IIc**—**IIIa** < **IIIb**. Compared with the

geometry of monomer, the lengths of N(1)—N(2), N (14)—N(15) and N(25)—N(26) decrease by 0.9— 2.4 pm, whereas the lengthes of N—O in the intermolec- ular interaction rings increase within 0.6 pm and 1.1 pm for dimers and trimers, respectively. The changes of bond lengths for dimers are less than those of trimers. The X— NO$_2$ (X = N, C, O) bond in nitro explosives is often re- ferred to as a detonation trigger.[15,33-35] The interaction causes the shortening of N—NO$_2$ bond for all clusters, especially for structure **IIIb**. It can be speculated that the interaction may lower the sensitivity in a certain degree. The bond angles and the dihedral angles of all five clus- ters change slightly from monomer, which implies that the influence of interaction on bond bending or internal rota- tion around single bond is very small.

I

IIa

IIb

IIc

IIIa

IIIb
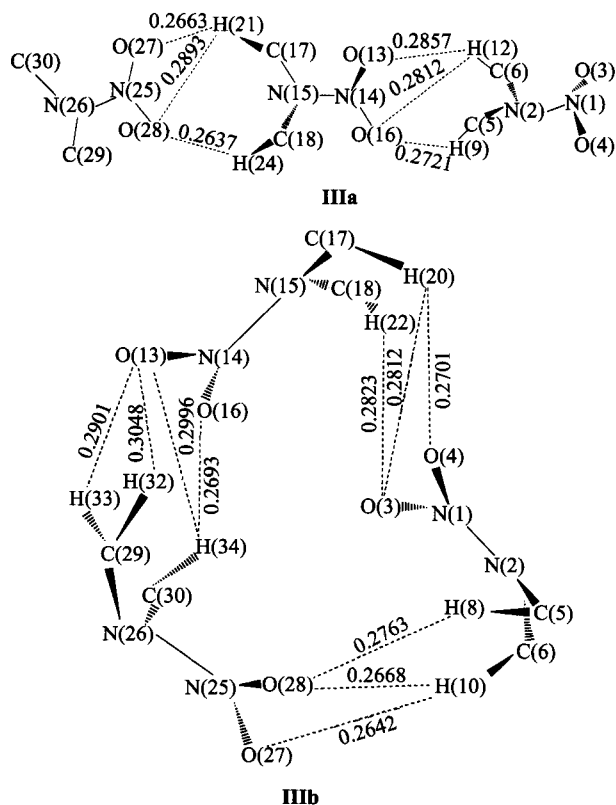
Fig. 1 Optimized structures, intermolecular distances (nm) and atomic numbering of DMNA and its clusters (only the intermolecular contact hydrogens are shown for trimers).

Atomic charges and charge transfer

Table 2 lists the atomic charges. The charge redis- tribution mainly occurs among the intermolecular contact- ing O ··· H atoms. Intermolecular contacting hydrogen atoms in dimers lose 0.0279 e—0.0422 e, whereas oxy- gen atoms which interact with the neighbor hydrogen atoms acquire 0.0046 e—0.0295 e. Intermolecular con- tacting hydrogen atoms in trimers lose 0.0059 e—0.0519 e, whereas oxygen atoms acquire 0.0059 e—0.0524 e. The changes of atomic charges in trimers are greater than those of dimers, showing the cooperativity effects in the interaction. The greatest changes of atomic charges are a- mong the atoms in **IIIb**, which is another evidence that intermolecular interaction in **IIIb** is relatively intense. For dimers, the net result of charge transfer is that a sub- molecule acquires 0.0118 e and 0.0192 e for **IIa** and **IIb**, respectively, whereas there is no net charge transfer for **IIc** due to the distances of their four O···H contacts being equal in pairs and their polarities in opposite direc-

Table 1 Optimized geometries of DMNA and its clusters at HF/6-31G* level (bond length in nm, bond angle and dihedral angle in degree)[a]

Clusters	Parameters and Values				
I	$R_{1\text{-}2}$ 0.1344	$R_{2\text{-}5}$ 0.1455	$\theta_{2\text{-}1\text{-}3}$ 117.41	$\theta_{2\text{-}5\text{-}7}$ 110.04	$\varphi_{3\text{-}1\text{-}2\text{-}6}$ −16.31
	$R_{1\text{-}3}$ 0.1197	$R_{5\text{-}7}$ 0.1077	$\theta_{1\text{-}2\text{-}5}$ 115.80	$\varphi_{3\text{-}1\text{-}2\text{-}4}$ 178.7	$\varphi_{3\text{-}1\text{-}2\text{-}5}$ −165.04
	$R_{5\text{-}9}$ 0.1079	$R_{5\text{-}8}$ 0.1085			
IIa	$R_{1\text{-}2}$ 0.1333	$R_{2\text{-}5}$ 0.1456	$R_{18\text{-}24}$ 0.1077	$R_{14\text{-}15}$ 0.1335	$\theta_{15\text{-}18\text{-}24}$ 106.99
	$R_{1\text{-}3}$ 0.1201	$R_{2\text{-}6}$ 0.1456	$R_{13\text{-}14}$ 0.1199	$R_{15\text{-}17}$ 0.1455	$\varphi_{3\text{-}1\text{-}2\text{-}4}$ 178.9
	$R_{1\text{-}4}$ 0.1200	$R_{17\text{-}21}$ 0.1077	$R_{14\text{-}16}$ 0.1199	$\theta_{15\text{-}17\text{-}21}$ 106.99	$\varphi_{13\text{-}14\text{-}16\text{-}15}$ 178.7
IIb	$R_{1\text{-}2}$ 0.1337	$R_{2\text{-}5}$ 0.1455	$R_{6\text{-}12}$ 0.1078	$R_{14\text{-}15}$ 0.1333	$\theta_{15\text{-}14\text{-}16}$ 117.67
	$R_{1\text{-}3}$ 0.1199	$R_{2\text{-}6}$ 0.1456	$R_{13\text{-}14}$ 0.1201	$R_{15\text{-}17}$ 0.1456	$\varphi_{3\text{-}1\text{-}2\text{-}4}$ 178.8
	$R_{1\text{-}4}$ 0.1199	$R_{5\text{-}9}$ 0.1078	$R_{14\text{-}16}$ 0.1199	$\theta_{2\text{-}6\text{-}12}$ 107.33	$\varphi_{13\text{-}14\text{-}16\text{-}15}$ 178.7
IIc	$R_{1\text{-}2}$ 0.1333	$R_{2\text{-}5}$ 0.1459	$R_{18\text{-}22}$ 0.1082	$R_{14\text{-}15}$ 0.1333	$\theta_{2\text{-}5\text{-}8}$ 111.68
	$R_{1\text{-}3}$ 0.1198	$R_{2\text{-}6}$ 0.1457	$R_{13\text{-}14}$ 0.1198	$R_{15\text{-}17}$ 0.1457	$\varphi_{3\text{-}1\text{-}2\text{-}4}$ 178.3
	$R_{1\text{-}4}$ 0.1203	$R_{5\text{-}8}$ 0.1082	$R_{14\text{-}16}$ 0.1203	$\theta_{2\text{-}1\text{-}4}$ 117.82	$\varphi_{13\text{-}14\text{-}16\text{-}15}$ 178.2
IIIa	$R_{1\text{-}2}$ 0.1333	$R_{5\text{-}9}$ 0.1077	$R_{15\text{-}17}$ 0.1457	$\theta_{1\text{-}2\text{-}6}$ 116.51	$\theta_{27\text{-}25\text{-}26}$ 117.75
	$R_{1\text{-}3}$ 0.1200	$R_{6\text{-}12}$ 0.1077	$R_{25\text{-}27}$ 0.1199	$\theta_{2\text{-}6\text{-}12}$ 107.06	$\varphi_{3\text{-}1\text{-}2\text{-}4}$ 178.9
	$R_{1\text{-}4}$ 0.1200	$R_{13\text{-}14}$ 0.1202	$R_{25\text{-}26}$ 0.1331	$\theta_{13\text{-}14\text{-}15}$ 117.91	$\varphi_{13\text{-}14\text{-}16\text{-}15}$ 178.9
	$R_{2\text{-}5}$ 0.1455	$R_{14\text{-}16}$ 0.1204	$R_{26\text{-}30}$ 0.1456	$\theta_{14\text{-}15\text{-}17}$ 117.00	$\varphi_{27\text{-}25\text{-}26\text{-}28}$ 179.0
	$R_{2\text{-}6}$ 0.1456	$R_{14\text{-}15}$ 0.1324	$\theta_{3\text{-}1\text{-}2}$ 117.57	$\theta_{15\text{-}17\text{-}21}$ 107.32	
IIIb	$R_{1\text{-}2}$ 0.1328	$R_{6\text{-}10}$ 0.1081	$R_{18\text{-}22}$ 0.1082	$\theta_{1\text{-}2\text{-}6}$ 116.46	$\theta_{25\text{-}26\text{-}30}$ 116.78
	$R_{1\text{-}3}$ 0.1204	$R_{13\text{-}14}$ 0.1202	$R_{25\text{-}26}$ 0.1320	$\theta_{2\text{-}6\text{-}10}$ 111.54	$\theta_{26\text{-}30\text{-}34}$ 111.47
	$R_{1\text{-}4}$ 0.1200	$R_{14\text{-}16}$ 0.1199	$R_{25\text{-}28}$ 0.1208	$\theta_{13\text{-}14\text{-}15}$ 117.70	$\varphi_{3\text{-}1\text{-}2\text{-}4}$ 177.9
	$R_{2\text{-}5}$ 0.1457	$R_{14\text{-}15}$ 0.1334	$R_{26\text{-}30}$ 0.1459	$\theta_{14\text{-}15\text{-}18}$ 115.85	$\varphi_{13\text{-}14\text{-}16\text{-}15}$ 177.7
	$R_{2\text{-}6}$ 0.1460	$R_{15\text{-}17}$ 0.1458	$R_{30\text{-}34}$ 0.1080	$\theta_{15\text{-}17\text{-}20}$ 111.48	$\varphi_{27\text{-}25\text{-}26\text{-}28}$ 178.9
	$R_{5\text{-}8}$ 0.1082	$R_{17\text{-}20}$ 0.1082	$\theta_{3\text{-}1\text{-}2}$ 117.92	$\theta_{27\text{-}25\text{-}26}$ 118.21	

Table 2 Atomic charges (in e) of DMNA and its clusters[a]

Atoms No.	I	IIa	IIb	IIc	IIIa	IIIb
N(1)	0.8306	0.8331	0.8304	0.8396	0.8308[0.8400]	0.8462[0.8446]
N(2)	−0.4426	−0.4424	−0.4432	−0.4346	−0.4453[−0.4440]	−0.4340[−0.4449]
O(3)	−0.5078	−0.5164	−0.5173	−0.5146	−0.5210[−0.5137]	−0.5435[−0.5232]
O(4)	−0.5078	−0.5158	−0.5188	−0.5372	−0.5224[−0.5261]	−0.5207[−0.5602]
C(5)	−0.2857	−0.2837	−0.2982	−0.3007	−0.2888[−0.2830]	−0.2875[−0.2731]
C(6)	−0.2858	−0.2838	−0.2991	−0.2884	−0.2900[−0.2837]	−0.2993[−0.2801]
H(7)	0.2265	0.2275	0.2138	0.2164	0.2077[0.2265]	0.2130[0.1987]
H(8)	0.1877	0.1951	0.1797	0.2299	0.1820[0.1968]	0.2193[0.2213]
H(9)	0.1854	0.1907	0.2196	0.1798	0.2167[0.1919]	0.1831[0.1913]
H(10)	0.1877	0.1953	0.1818	0.2087	0.1835[0.1966]	0.2396[0.2320]
H(11)	0.2266	0.2280	0.2117	0.2177	0.2065[0.2275]	0.2106[0.2020]
H(12)	0.1854	0.1906	0.2205	0.1835	0.2200[0.1919]	0.1795[0.1892]
O(13)	(−0.5078)	−0.5189	−0.5221	−0.5146	−0.5260	−0.5333
N(14)	(0.8306)	0.8308	0.8395	0.8396	0.8328	0.8453
N(15)	(−0.4426)	−0.4443	−0.4441	−0.4346	−0.4425	−0.4362
O(16)	(−0.5078)	−0.5192	−0.5123	−0.5372	−0.5291	−0.5172
C(17)	(−0.2857)	−0.2898	−0.2833	−0.2884	−0.2983	−0.3021
C(18)	(−0.2858)	−0.2898	−0.2836	−0.3007	−0.2944	−0.2882
H(19)	(0.2265)	0.2106	0.2277	0.2177	0.2129	0.2126
H(20)	(0.1877)	0.1828	0.1943	0.2087	0.1887	0.2300
H(21)	(0.1854)	0.2133	0.1905	0.1835	0.2280	0.1780
H(22)	(0.1877)	0.1827	0.1948	0.2299	0.1876	0.2118
H(23)	(0.2266)	0.2101	0.2276	0.2165	0.2153	0.2157
H(24)	(0.1854)	0.2134	0.1904	0.1798	0.2248	0.1798

[a] Charges in parentheses are of monomer, data in square brackets refer to atomic numbers 25—36 of the third submolecule.

tion. For trimers, the net result of charge transfer is that a submolecule at the end of the chain structure acquires 0.0204 e for **IIIa**, whereas there is approximately no net charge transfer for **IIIb** due to its cyclic contacting. The dipole moments of the clusters are 10.920 D, 10.790 D, 0.000 D, 16.270 D and 3.51 D for **IIa**, **IIb**, **IIc**, **IIIa** and **IIIb**, respectively, which are about the sum of monomer's 4.85 D for **IIa**, **IIb** and **IIIa**.

Vibrational frequencies and their shifts

The simulated infrared (IR) spectra for the DMNA clusters are shown in Fig. 2 where the intensities (KM/mol) are plotted against the harmonic vibrational frequencies (cm^{-1}). The frequencies with intensities larger than 500 KM/mol are associated with N—O stretches or wags that exhibit large dipole moment changes. These two intense frequencies exhibit slight red shifts (within -19 cm^{-1}) with respect to those of its monomer, accompanied by the increasing of intensities. The shifts demonstrate that the N—O bonds are somewhat weakened. Whereas there are slight blue shifts (within $+15$ cm^{-1}) in the ranges of 3230—3390 cm^{-1}, these modes are associated with the motion of hydrogen atoms of the methyl group. Also, the mode of $ca.$ 1670 cm^{-1} associated with C—H rocking exhibits some blue shifts. The blue shifts may be caused by the field effect of the intermolecular oxygen contacting. It is known that the normal hydrogen bonding causes a large red shift in the X—H (X = O, N, F or Cl) stretch frequency. Therefore, the H-bonding effect is negligible in these clusters.

Interaction energies and cooperative effects

Table 3 gives both the uncorrected and corrected interaction energies and the contributions of cooperativity. There are no imaginary frequencies for all structures in Table 3, which convicts that all the structures in Fig. 1 correspond minima on their potential energy surfaces. The interaction energies after being corrected for BSSE and ZPE demonstrate that the stability order for the clusters is **IIa** —**IIb** < **IIc** < **IIIa** < **IIIb**.

Although MP4SDTQ gives much more accurate electron correlation energy, MP2 is also a preferable method for this purpose on general large systems for which the MP4 method is computationally expensive or impractical.[11] At the MP2/6-31G* //HF/6-31G* level, the pro-

portion of correlated interaction energies to their total interaction energies (viz. $[\Delta E(MP2)-\Delta E(HF)]/\Delta E(MP2)$, see data in parentheses of Table 3) for all clusters is at least 29.3 percent, so it is imperative to include the electron correlation energies into interaction energies. The discrepancies between $\Delta E(MP2)_C$ and $\Delta E(MP2)$ are 11.0, 10.0, 19.8, 21.8 and 37.3 kJ/mol for **IIa**, **IIb**, **IIc**, **IIIa** and **IIIb**, respectively, indicating that it is also necessary to correct the BSSE. The ZPE corrections for the interaction energies are much less than those of BSSE. The BSSE and ZPE corrected interaction energies of the most stable dimer and trimer are -24.68 kJ/mol and -47.27 kJ/mol, respectively, at the MP2/6-31G* //HF/6-31G* level. Based on the changes of binding energies upon addition of a new molecule to a cluster, the transition from the dimer to the trimer involves the contributions of cooperativity. The cyclic trimer displays more cooperative effects than the chain trimer.
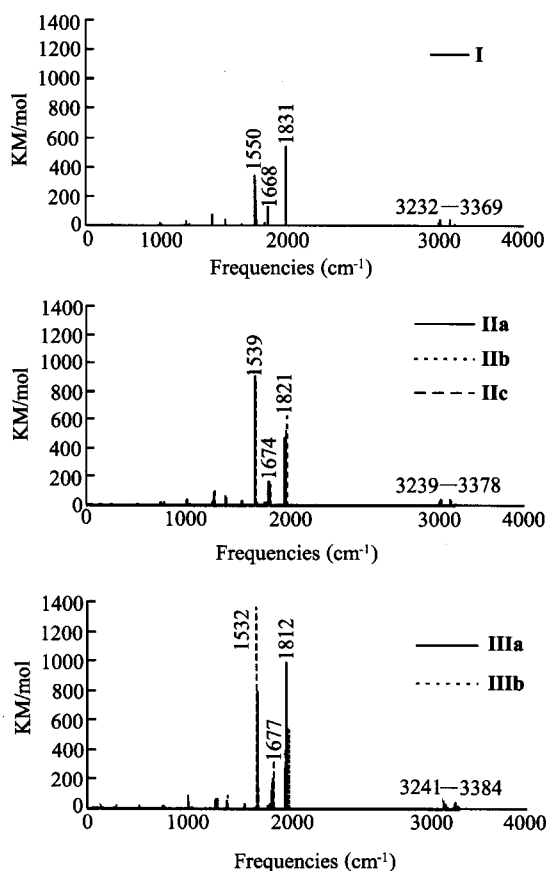

Fig. 2 Calculated IR intensities (KM/mol) against frequencies (cm^{-1}) for the DMNA and its clusters.

In addition, Table 3 also shows the interaction ener-

gies at the MP2/6-311G*//HF/6-31G* level to verify the suitability of basis function. Both the uncorrected and corrected interaction energies are rather close to those using the 6-31G* basis set. Therefore, the 6-31G* basis set is suitable for the systems studied here, and the discussion above and thereafter is derived from the optimized structures by using this basis set.

Natural bond orbital and Mulliken populations

The donor and the acceptor of NBO between inter-

molecules, and their interacting stable energies obtained from MP2 analysis of Fock matrix in NBO basis are collected in Table 4. The stable energies are proportional to the NBO interacting intensities. All the oxygen atoms donate their lone pairs to the neighbor C—H antibonds, which strengthen the intermolecular O···H interactions. For dimers, the NBO interacting in **IIb** is greater than that in **IIa** or **IIc**, although **IIc**'s intermolecular distances are very close to those of **IIb**. It demonstrates the main contribution to **IIc**'s interaction energy is from the dispersion and/or electrostatic force. The biggest NBO stable

Table 3   Interaction energies and cooperative energies for DMNA clusters (kJ/mol)^a

Basis sets	Energies	IIa	IIb	IIc	IIIa	IIIb
6-31G*	ΔE(HF)	− 17.26	− 17.07	− 29.42	− 37.91	− 55.89
	ΔE(MP2)	− 24.70(30.1)	− 24.30(29.8)	− 48.21(39.0)	− 53.62(29.3)	− 91.14(38.7)
	ΔE(HF)$_\text{C}$	− 11.40	− 12.19	− 18.12	− 26.85	− 35.51
	ΔE(MP2)$_\text{C}$	− 13.73	− 14.32	− 28.37	− 31.87	− 53.89
	ΔE(MP2)$_\text{C,ZPE}$	− 12.30	− 12.77	− 24.68	− 28.72	− 47.27
	$E_\text{nopair,MP2}$				− 1.50	− 2.97
6-311G*	ΔE(HF)	− 16.66	− 17.01	− 29.02	− 37.15	− 55.50
	ΔE(MP2)	− 23.71	− 23.41	− 46.58	− 51.22	− 88.74
	ΔE(HF)$_\text{C}$	− 10.87	− 11.94	− 18.75	− 25.81	− 36.15
ΔE(MP2)$_\text{C}$		− 12.09	− 13.01	− 26.98	− 28.49	− 50.89

^{a} The values in parentheses represent $[\Delta E(\text{MP2}) - \Delta E(\text{HF})]/\Delta E(\text{MP2}) \times 100$.

Table 4   Intermolecular natural bond orbital interacting and the corresponding stable energy (kJ/mol)^a

Dimers	Donor	Acceptor (BD*)	E	Trimers	Donor	Acceptor (BD*)	E
IIa	LP(1) O(3)	C(17)—H(21)	0.63	**IIIa**	LP(1) O(27)	C(17)—H(21)	1.34
	LP(1) O(3)	C(18)—H(24)	0.59		LP(2) O(27)	C(17)—H(21)	3.85
	LP(2) O(3)	C(17)—H(21)	1.80		LP(1) O(28)	C(18)—H(24)	2.59
	LP(2) O(3)	C(18)—H(24)	1.80		LP(2) O(28)	C(17)—H(21)	1.09
	LP(2) O(4)	C(17)—H(21)	0.79		LP(2) O(28)	C(18)—H(24)	3.14
	LP(2) O(4)	C(18)—H(24)	0.92		LP(2) O(13)	C(5)—H(9)	1.26
IIb	LP(1) O(13)	C(5)—H(9)	2.43		LP(2) O(13)	C(6)—H(12)	0.92
	LP(2) O(13)	C(5)—H(9)	3.01		LP(1) O(16)	C(5)—H(9)	0.63
	LP(1) O(16)	C(6)—H(12)	1.17		LP(2) O(16)	C(5)—H(9)	2.26
	LP(2) O(16)	C(6)—H(12)	3.31		LP(2) O(16)	C(6)—H(12)	2.13
IIc	LP(1) O(3)	C(18)—H(22)	0.84	**IIIb**	LP(1) O(16)	C(30)—H(34)	1.13
	LP(2) O(3)	C(18)—H(22)	1.84		LP(2) O(16)	C(30)—H(34)	2.22
	LP(2) O(4)	C(18)—H(22)	0.79		LP(1) O(3)	C(18)—H(22)	1.51
	LP(1) O(13)	C(5)—H(8)	0.84		LP(2) O(3)	C(17)—H(20)	1.13
	LP(2) O(13)	C(5)—H(8)	1.84		LP(1) O(4)	C(17)—H(20)	1.17
	LP(2) O(16)	C(5)—H(8)	0.79		LP(2) O(4)	C(17)—H(20)	3.64
					LP(1) O(27)	C(6)—H(10)	1.09
					LP(2) O(27)	C(6)—H(10)	2.59
					LP(1) O(28)	C(5)—H(8)	1.34
					LP(2) O(28)	C(6)—H(10)	1.21

^{a} LP means lone pair; BD* represents antibond.

energy in dimers derives from the interacting between O (16)'s lone pair as a donor and C(6)—H(12) antibond as an acceptor in **IIb**, although O(16)···H(12) is not the shortest intermolecular distance for all dimers, which may be due to its suitable overlap orientation. The NBO interacting in trimer is generally greater than that in dimer. The NBO stable energies in the two trimers are roughly the same.

Apart from the NBO analyses, the Mulliken population of intermolecular O···H is also relevant to reveal the essential of intermolecular interaction. The Mulliken populations of O ··· H contacts are as follows: 0.0029— 0.0057 for **IIa**, 0.0066—0.0080 for **IIb**, 0.0032— 0.0062 for **IIc**, 0.0039—0.0088 for **IIIa** and 0.0017— 0.0084 for **IIIb**. All the values above are much less than that of a normal H-bonding, which reveals again that the

dispersion and/or electrostatic force, other than the H-bonding, is dominant in DMNA clusters, and which also demonstrates that the interaction in trimer is more intensive than in dimer.

Thermodynamic properties

On the basis of vibrational analysis and statistical thermodynamic, the standard thermodynamic functions, heat capacities (C_P^0), entropies (S_m^0) and enthalpies (H_m^0), were obtained and listed in Table 5. The magnitudes of C_P^0 with the same number of molecules are approximately the same at each temperature, but are larger than two or three times of **I**'s C_P^0 by 14.3—16.8 J/(mol· K^{-1}) and 29.9—33.0 J/(mol· K^{-1}) at 200—800 K, for dimers and trimers respectively. In the course of monomer

Table 5 Thermodynamic properties of DMNA and its clusters at different temperatures[a]

Structure	Temp. (K)	C_P^0 (J/mol·K^{-1})	S_m^0 (J/mol·K^{-1})	H_m^0 (kJ/mol)	ΔS_T (J/mol·K^{-1})	ΔH_T (kJ/mol)	ΔG_T (kJ/mol)
I	200.00	74.99	294.74	10.73			
	298.15	93.19	328.01	18.97			
	400.00	113.85	358.26	29.51			
	600.00	151.75	411.84	56.20			
	800.00	180.78	459.68	89.59			
IIa	200.00	166.76	498.99	23.93	− 90.49	− 14.79	3.31
	298.15	202.96	572.19	42.04	− 83.83	− 13.16	11.83
	400.00	244.18	637.55	64.80	− 78.97	− 11.48	20.11
	600.00	319.95	751.39	121.47	− 72.29	− 8.19	35.18
	800.00	378.01	851.80	191.56	− 67.56	− 4.88	49.17
IIb	200.00	166.76	498.99	23.93	− 90.49	− 14.60	3.50
	298.15	202.96	572.19	42.04	− 83.83	− 12.97	12.02
	400.00	244.18	637.55	64.80	− 78.97	− 11.29	20.30
	600.00	319.95	751.39	21.47	− 72.29	− 8.00	35.37
	800.00	378.01	851.80	191.56	− 67.56	-4.69	49.36
IIc	200.00	164.31	444.43	22.32	− 145.05	− 28.56	0.45
	298.15	201.80	516.94	40.26	− 139.08	− 27.10	14.37
	400.00	243.58	582.03	62.93	− 134.49	− 25.51	28.29
	600.00	319.76	695.74	119.53	− 127.94	− 22.29	54.47
	800.00	377.91	796.10	189.59	− 123.26	− 19.01	79.60
IIIa	200.00	257.95	698.50	36.97	− 185.72	− 33.13	4.01
	298.15	312.47	811.47	64.92	− 172.56	− 29.90	21.55
	400.00	374.37	911.87	99.87	− 162.91	− 26.57	38.59
	600.00	488.09	1085.95	186.51	− 149.57	− 20.00	69.74
	800.00	575.21	1238.91	293.27	− 140.13	− 13.41	98.69
IIIb	200.00	254.86	600.66	34.58	− 283.56	− 53.50	3.21
	298.15	311.01	712.75	62.32	− 271.28	− 50.48	30.40
	400.00	373.64	812.84	97.16	− 261.94	− 47.26	57.52
	600.00	487.87	986.73	183.72	− 248.79	− 40.77	108.50
	800.00	575.07	1139.65	290.45	− 239.39	− 34.21	157.30

[a] $\Delta S_T = (S_m^0)_i - n(S_m^0)_I$, $\Delta H_T = (H_m^0 + E_{HF} + ZPE)_i - n(H_m^0 + E_{HF} + ZPE)_I$ (i = II, III with n = 2,3 respectively),

$\Delta G_T = \Delta H_T - T\Delta S_T$, and no scale factor for frequencies is imposed.

to clusters, both the entropy and the enthalpy decrease at any temperature from 200.0 K to 800.0 K. The decrease of **IIc**'s entropy is much more than that of **IIa** or **IIb** which is apparently due to its higher symmetry (C_i) and therefore less disorder. The decrease of **IIIb**'s entropy is much more than that of **IIIa** due to its cyclic structure and more intermolecular contacts. The intermolecular interaction is therefore an exothermic process accompanied by a decrease in the probability, and the interactions weaken as temperature increases. The order of $(\Delta H_T)_{\text{IIa}}$—$(\Delta H_T)_{\text{IIb}} > (\Delta H_T)_{\text{IIc}}$ —$(\Delta H_T)_{\text{IIIa}} > (\Delta H_T)_{\text{IIIb}}$ also gives the same interacting sequence of **IIa** —**IIb** < **IIc** —**IIIa** < **IIIb** as the interaction energies, except that the value of $(\Delta H_T)_{\text{IIc}}$ is much less than that of $(\Delta H_T)_{\text{IIIa}}$ at 800 K. From equation $\Delta G = \Delta H - T\Delta S$, the changes of Gibbs free energies (ΔG) in the processes $\text{I} \rightarrow \text{IIc}$ and $\text{I} \rightarrow \text{IIIb}$ are 14.37 kJ/mol and 30.40 kJ/mol, respectively, at 298.15 K according to the calculation model of ideal-gas. Since the difference of the ΔH_T values between the dimers or trimers is not large, the effect of entropy changes the above stability order, $i.e.$ the ΔG_T value gives different stability order from that of ΔH_T. At lower temperature, ΔG_T establishes the stability sequence **IIa** —**IIb** —**IIIa** —**IIIb** < **IIc**, but **IIa** —**IIb** > **IIc** > **IIIa** > **IIIb** at higher temperature, which is only applicable for ideal-gas systems.

Conclusions

From *ab initio* calculations in the paper, the following conclusions can be drawn:

(1) The interacting energies of the DMNA clusters is **IIa** —**IIb** < **IIc** —**IIIa** < **IIIb**. There exist cooperative effects in the trimers, especially in cyclic **IIIb**.

(2) The dispersion and/or electrostatic force, other than the H-bonding, are dominant in DMNA clusters.

(3) The interaction is an exothermic process with the probability decreasing. The changes of both entropy and enthalpy on going from the monomer to the dimers increase as temperature decreases, but the changes of free energy decrease as temperature decrease.

References

1   Scheiner, S. *Theoretic Models of Chemical Bonding*, Ed.: Maksic, Z. B., Springer-Verlag, Berlin, **1991**, p. 173.

2   Wang, Y.-B.; Tao, F.-M.; Pan, Y.-K. *J. Mol. Struct.* (*THEOCHEM*) **1994**, *309*, 235.

3   Zhang, Y.; Wang, Y.-B.; Sun, Z.-M.; Tian, A.-M. *Chem. J. Chin. Univ.* **2000**, *21*, 99 (in Chinese).

4   Hobza, P.; Selzle, H. L.; Schlag, E. W. *Chem. Rev.* **1994**, *94*, 1767.

5   Sauer, J.; Ugliego, P.; Garrone, E.; Saunders, V. R. *Chem. Rev.* **1994**, *94*, 2095.

6   Chalasiński, G.; Szczśniak, M. M. *Chem. Rev.* **1994**, *94*, 1723.

7   Cabaleiro-Lago, E. M.; Rios, M. A. *J. Phys. Chem. A* **1999**, *103*, 6468.

8   Li, J. S.; Xiao, H. M.; Dong, H. S. *Int. J. Quantum Chem.* **2000**, *78*, 94.

9   Li, J. S.; Xiao, H. M.; Dong, H. S. *Propellants Explos., Pyrotec.* **2000**, *25*, 26.

10   Li, J. S.; Xiao, H. M. *Acta Phys.-Chim. Sin.* **2000**, *16*, 36 (in Chinese).

11   Li, J. S.; Xiao, H. M.; Dong H. S. *Chin. J. Chem.* **2000**, *18*, 815.

12   Xiao, H. M.; Li, J. S.; Dong H. S. *Acta Chim. Sinica* **2000**, *58*, 297 (in Chinese).

13   Xiao, H. M.; Li, J. S.; Dong, H. S. *J. Phys. Org. Chem.* **2001**, *14*, 644.

14   Elrod, M. J.; Saykally, R. J. *Chem. Rev.* **1994**, *94*, 1975.

15   Delpuech, A.; Cherville, J. *Propellants Explos.* **1978**, *3*, 169.

16   Sumpter, B. G.; Thompson, D. L. *J. Chem. Phys.* **1988**, *88*, 6889.

17   Fan, K.-N.; Xiao, H.-M.; Li, Y.-F. *Acta Chim. Sinica* **1989**, *47*, 952 (in Chinese).

18   Ling, Y.; Tang, Z. H.; Xiao, H. M. *Propellants Explos., Pyrotec.* **1992**, *17*, 116.

19   Habibollahzadeh, D.; Murray, J. S.; Redfern, P. C.; Politzer, P. *J. Phys. Chem.* **1991**, *95*, 7703.

20   Harris, J. N.; Lammertsma, K. *J. Phys. Chem. A* **1997**, *101*, 1370.

21   Smith, G. D.; Bharadwaj, R. K.; Bedrov, D.; Ayyagari, C. *J. Phys. Chem B* **1999**, *103*, 705.

22   Schlegel, H. B. *J. Comput. Chem.* **1982**, *3*, 214.

23   Fletcher, R.; Powell, M. J. D. *Comput. J.* **1963**, *6*, 163.

24   Raghavachari, K.; Pople J. A.; Replogle, E. S.; Head-Gordon, M. *J. Phys. Chem.* **1990**, *94*, 5579.

25   McDouall, J. J.; Peasley, K.; Robb, M. A. *Chem. Phys. Lett.* **1988**, *148*, 183.

26   Binkley, J. S.; Pople, J. A. *Int. J. Quantum Chem.* **1975**, *9*, 229.

27   Boys, S. F.; Bernardi, F. *Mol. Phys.* **1970**, *19*, 553.

28   Johnson, A.; Kollman, P.; Rothenberg, S. *Theor. Chem. Acta* **1973**, *29*, 167.

29   Chalasinski, G.; Szczesniak, M. M. *Mol. Phys.* **1988**, *63*, 205.

30   Frisch, M. J.; Trucks, G. W.; Schlegel, H. B.; Scuseria,

G. E.; Robb, M. A.; Cheeseman, J. R.; Zakrzewski, V.
G.; Montgomery, J. A.; Stratmann, R. E.; Burant, J. C.;
Dapprich, S.; Millam, J. M.; Daniels, A. D.; Kudin, K.
N.; Strain, M. C.; Farkas, O.; Tomasi, J.; Barone, V.;
Cossi, M.; Cammi, R.; Mennucci, B.; Pomelli, C.;
Adamo, C.; Clifford, S.; Ochterski, J.; Petersson, G. A.;
Ayala, P. Y.; Cui, Q.; Morokuma, K.; Malick, D. K.;
Rabuck, A. D.; Raghavachari, K.; Foresman, J. B.;
Cioslowski, J.; Ortiz, J. V.; Stefanov, B. B.; Liu, G.;
Liashenko, A.; Piskorz, P.; Komaromi, I.; Gomperts, R.;
Martin, R. L.; Fox, D. J.; Keith, T.; Al-Laham, M. A.;
Peng, C. Y.; Nanayakkara, A.; Gonzalez, C.; Challa-
combe, M.; Gill, P. M. W.; Johnson, B. G.; Chen, W.;
Wong, M. W.; Andres, J. L.; Head-Gordon, M.; Re-

plogle, E. S.; Pople, J. A. *Gaussian 98*, Revision A.7,
Gaussian In., Pittsburgh PA, **1998**.

31   Stolevik, R.; Rademacher, P. *Acta Chem. Scand.* **1969**,
23, 672.

32   Filhol, A.; Bravic, G.; Rey-Lafon, M.; Thomas, M. *Acta
Crystallogr B* **1980**, *36*, 575.

33   Xiao, H.-M.; Wang, Z.-Y.; Yao, J.-M. *Acta Chim. Sini-
ca* **1985**, *43*, 14 (in Chinese).

34   Xiao, H.-M. *Molecular Orbital Theory for Nitro Compounds*,
National Defense Industrial Press, Beijing, **1993**, pp. 181—
217 (in Chinese).

35   Xiao, H.-M.; Fan, J.-F.; Gu, Z.-M.; Dong, H.-S.
Chem. Phys. **1998**, *226*, 15.